Thermochimica Acta 514 (2011) 1–9

Contents lists available at ScienceDirect

Thermochimica Acta

journal homepage: www.elsevier.com/locate/tca

Thermodynamics of mixtures containing oxaalkanes. 6. Random mixing in ether + benzene, or + toluene systems

Juan Antonio González*, Isaías García De La Fuente, José Carlos Cobos, Ismael Mozo, Iván Alonso

G.E.T.E.F., Departamento de Física Aplicada, Facultad de Ciencias, Universidad de Valladolid, 47071 Valladolid, Spain

ARTICLE INFO

Article history:
Received 18 October 2010
Received in revised form
17 November 2010
Accepted 19 November 2010
Available online 30 November 2010

Keywords:
Flory
Ether
Aromatic
Interactions
Steric effects
Cyclization
Random mixing

ABSTRACT

The Flory model has been applied to linear or cyclic ether + benzene, or +toluene mixtures. In addition, the relative variation of the molar excess enthalpy, H^E_m, along homologous series of the considered systems, has been discussed taking into account the contributions to H^E_m from the ether–ether, aromatic–aromatic and ether–aromatic interactions. It has been shown that in $CH_3(CH_2)_{u-1}O(CH_2CH_2O)_v(CH_2)_{u-1}CH_3$ + benzene mixtures, the u increase (v fixed) leads to a weakening of interactions between unlike molecules, and that proximity effects also weaken this type of interactions. In contrast, the v increase (u fixed) or cyclization lead to stronger interactions between unlike molecules. From the application of the model, it is concluded that the random mixing hypothesis may be considered to be valid to a large extent for many of the investigated solutions. Erroneously, strong orientational effects are predicted for 1,3-dioxolane, or 1,4-dioxane + benzene systems, but this has been attributed to the model can not describe asymmetric H^E_m curves when the mixture compounds show close values for V_i (molar volume) and for V^*_i (reduction parameter for volume). Previous calculations on the basis of the Kirkwood–Buff integrals formalism confirm that the mixture structure is close to random mixing. Flory results on the excess molar volumes have been discussed taking into account the so-called curvature and P^* contributions to this excess function.

1. Introduction

It is known that the Flory model [1] is commonly used to describe simultaneously, excess molar enthalpies, H^E_m, and excess molar volumes, V^E_m, of systems formed by non-polar (benzene [2]) or slightly polar compound (N,N,N-trialkylamine [3] or monoether [4]) and alkane, or involving two polar compounds as 1-alkanol + 1-alkanol [5] or 2-methoxyethanol + hydroxyether [6]. The good agreement between experimental and theoretical results implies that the random mixing hypothesis, a basic assumption of the Flory model, is attained in large extent for these systems. It may be due to such solutions are characterized by dispersive interactions (benzene + alkane), or by weak dipolar interactions (monoether + alkane) or to the identical chemical nature of the two mixture compounds (1-alkanol + 1-alkanol). In addition, the Flory model has also been widely used to investigate order creation and order destruction processes in binary mixtures formed by one alkane and one non-polar or slightly polar compound, with spherical or plate like shape [7–10]. As any order effects are ignored in the theory (random mixing hypothesis), differences between experimental values for the magnitudes H^E_m, V^E_m, C^E_{pm}, $(\partial V^E_m/\partial T)_p$, or $-(\partial V^E_m/\partial P)_T$ and the corresponding Flory results are ascribed to order effects. The main conclusion of these studies is the existence of a short orientational order in long chain alkanes, which does not appear in highly branched isomeric alkanes, or short chain alkanes.

The theory has been also applied to predict isobaric expansion coefficient, α_P isentropic, κ_S, or isothermal, κ_T compressibilities and speeds of sound, u, of simple systems, as those involving two alkanes, or of the type cyclohexane or benzene + n-alkane [2,11,12]. We have shown that the model application can be extended in two ways. Firstly, the theory provides rather accurate predictions on α_P, κ_S, κ_T and u of complex mixtures as alkoxyethanol + dibutylether, or +1-butanol [13]. Secondly, it is possible to investigate the existence of orientational effects in complex mixtures by studying the variation of the interaction parameter, X_{12}, with the composition [14,15]. Here, in order to gain insight into the interactions and structure of ether + aromatic compound mixtures, the same method is applied to investigate the validity of the random mixing hypothesis in ether + benzene or + toluene mixtures. Previously, as similar research has been presented for ether + alkane systems [16].

From a practical point of view, this type of studies is particularly interesting as precise molecular recognition is essential to living systems [17]. Thus, biological discriminations as enzyme–substrate or antigen–antibody are well known. In chemical systems, molecular recognition has been extensively studied using a variety of model compounds such as 1,3-dioxane or crown ethers [17,18].

* Corresponding author. Tel.: +34 983 423757; fax: +34 983 423136.
E-mail address: jagl@termo.uva.es (J.A. González).

0040-6031/$ – see front matter © 2010 Elsevier B.V. All rights reserved.
doi:10.1016/j.tca.2010.11.023

Actually, it is accepted that molecular recognition, biological or chemical, is due to specific weak interactions between the interacting groups of the respective molecules [17]. Mixtures containing ethers are also important because they are increasingly used as additives to gasoline owing to their octane-enhancing and pollution-reducing properties [19,20]. In addition, cyclic polyethers have attracted interest as model substances for bio-systems (see above), separation techniques, chemical analysis or in relation to their use in synthetic methods in organic chemistry [21,22]. In the case of crown ethers, this is due to the fact that they can selectively form strong electrostatic complexes with a large variety of ligands in different solvents [23–25].

2. The Flory model

In this section, a brief summary of the model is presented. More details are given in the original works [1,26–29]. The main features of the theory are as follows: (i) molecules are divided into segments. A segment is an arbitrarily chosen isomeric portion of the molecule. The number of segments per molecule of component i is denoted by r_i and the number of intermolecular contact sites per segment by s_i. (ii) The mean intermolecular energy per contact is proportional to $-\eta/v_s$ (where η is a positive constant characterizing the energy of interaction for a pair of neighbouring sites and v_s is the volume of a segment). (iii) When stating the configurational partition function, it is assumed that the number of external degrees of freedom of the segments is lower than 3, in order to take into account the restrictions on the precise location of a given segment by its neighbours in the same chain. (iv) Random mixing is assumed: the probability of having species of kind i neighbours to any given site is equal to the site fraction, θ_i ($\theta_i = s_i r_i N_i / srN$; where $N = N_1 + N_2$ is the total number of molecules and r and s are the total number of intermolecular segments and contact sites per segment, respectively). For very large total number of contact sites, the probability of formation of an interaction between contacts sites belonging to different liquids is $\theta_1\theta_2$. Under these hypotheses, the Flory equation of state is given by:

$$\frac{\tilde{P}\tilde{V}}{\tilde{T}} = \frac{\tilde{V}^{1/3}}{\tilde{V}^{1/3}-1} - \frac{1}{\tilde{V}\tilde{T}} \tag{1}$$

where $\tilde{V} = V/V^*$; $\tilde{P} = P/P^*$ and $\tilde{T} = T/T^*$ are the reduced volume, pressure and temperature, respectively. Eq. (1) is valid for pure liquids and liquid mixtures. For pure liquids, the reduction parameters, V_i^*, P_i^* and T_i^* can be obtained from experimental data, such as α_{Pi} and κ_{Ti}. For mixtures, the corresponding parameters are calculated as follows:

$$V^* = x_1 V_1^* + x_2 V_2^* \tag{2}$$

$$T^* = \frac{\varphi_1 P_1^* + \varphi_2 P_2^* - \varphi_1\theta_2 X_{12}}{\varphi_1 P_1^*/T_1^* + \varphi_2 P_2^*/T_2^*} \tag{3}$$

$$P^* = \varphi_1 P_1^* + \varphi_2 P_2^* - \varphi_1\theta_2 X_{12} \tag{4}$$

In Eqs. (3) and (4), $\varphi_i = x_i V_i^* / \sum x_i V_i^*$ is the segment fraction and θ_2 is alternatively calculated as: $\theta_2 = \varphi_2/(\varphi_2 + S_{12}\varphi_1)$. S_{12} is the so-called geometrical parameter of the mixture, which, assuming that the molecules are spherical, is calculated as $S_{12} = (V_1^*/V_2^*)^{-1/3}$. The energetic parameter, X_{12}, also present in Eqs. (3) and (4), is defined by similarity with:

$$P_i^* = \frac{s_i \eta_{ii}}{2 v_s^{*2}} \tag{5}$$

as

$$X_{12} = \frac{s_1 \Delta\eta}{2 v_s^{*2}} \tag{6}$$

where $\Delta\eta = \eta_{11} + \eta_{22} - 2\eta_{12}$. In Eqs. (5) and (6), v_s^* (reduction volume for segment) and η_{ij} are changed from molecular units to molar units per segments. H_m^E is determined from:

$$H_m^E = \frac{x_1 V_1^* \theta_2 X_{12}}{\tilde{V}} + x_1 V_1^* P_1^* \left(\frac{1}{\tilde{V}_1} - \frac{1}{\tilde{V}}\right) + x_2 V_2^* P_2^* \left(\frac{1}{\tilde{V}_2} - \frac{1}{\tilde{V}}\right) \tag{7}$$

which can be also written as:

$$H_m^E = \frac{x_1 V_1^* \theta_2 X_{12}}{\tilde{V}} + x_1 V_1^* \varphi_2 \left(\frac{\tilde{V}_1 - \tilde{V}_2}{\tilde{V}_o}\right)\left(\frac{P_2^*}{\tilde{V}_2} - \frac{P_1^*}{\tilde{V}_1}\right) + \frac{V_m^E}{(\tilde{V}_o)^2(\varphi_1 P_1^* + \varphi_2 P_2^*)} \tag{8}$$

where $\tilde{V}_0 = \varphi_1\tilde{V}_1 + \varphi_2\tilde{V}_2$. The term which depends directly on X_{12} in Eq. (8) is usually named the interaction contribution [26] to H_m^E. The remaining terms are the so-called equation of state contribution [26] to H_m^E. The reduced volume of the mixture, $\tilde{V}$, in Eqs. (7) and (8) is obtained from the equation of state. Therefore, the molar excess volume can be also calculated:

$$V_m^E = (x_1 V_1^* + x_2 V_2^*)(\tilde{V} - \varphi_1\tilde{V}_1 - \varphi_2\tilde{V}_2) \tag{9}$$

3. Estimation of the Flory interaction parameter

X_{12} can be determined from a H_m^E measurement at a given composition from the equation [14,15]:

$$X_{12} = \frac{x_1 P_1^* V_1^* (1 - \tilde{T}_1/\tilde{T}) + x_2 P_2^* V_2^* (1 - \tilde{T}_2/\tilde{T})}{x_1 V_1^* \theta_2} \tag{10}$$

For the use of this expression, it must be taken into account that $\tilde{V}\tilde{T}$ is a function of H_m^E:

$$H_m^E = \frac{x_1 P_1^* V_1^*}{\tilde{V}_1} + \frac{x_2 P_2^* V_2^*}{\tilde{V}_2} + \frac{1}{\tilde{V}\tilde{T}}(x_1 P_1^* V_1^* \tilde{T}_1 + x_2 P_2^* V_2^* \tilde{T}_2) \tag{11}$$

and that, from the equation of state, $\tilde{V} = \tilde{V}(\tilde{T})$. For normal applications, it is possible to use the so-called $\tilde{p} \approx 0$ approximation of the equation of state, which is a good approximation at atmospheric pressure. More details have been given elsewhere [14,15]. Eq. (10) generalizes that previously given to calculate X_{12} from H_m^E at $x_1 = 0.5$ [30]. Properties of the pure compounds at 298.15 K, molar volumes, α_{Pi} and κ_{Ti}, and the corresponding reduction parameters, P_i^* and V_i^* ($i = 1, 2$), needed for calculations are listed in Table 1. Values of these properties at $T \neq 298.15$ K were estimated according to the method used previously [16]. X_{12} values determined from experimental H_m^E data at $x_1 = 0.5$ are collected in Table 2.

4. Results

Results on H_m^E and V_m^E obtained from the Flory model using X_{12} values at $x_1 = 0.5$ are listed in Tables 2 and 3, respectively. A comparison between experimental and theoretical values for H_m^E and V_m^E are shown graphically in Figs. 1–4. For the sake of clarity, Table 2 also includes the relative standard deviations for H_m^E defined as:

$$\sigma_r(H_m^E) = \left[\frac{1}{N}\sum\left(\frac{H_{m,\,exp}^E - H_{m,\,calc}^E}{H_{m,\,exp}^E}\right)^2\right]^{1/2} \tag{12}$$

where $N = 19$ is the number of data points, and $H_{m,\,exp}^E$ represents smoothed H_m^E values calculated at $\Delta x_1 = 0.05$ in the composition range [0.05, 0.95] from polynomial expansions given in the original works. In order to obtain detailed information on the concentration dependence of X_{12}, this magnitude has been determined using Eq.

Table 1
Flory parameters[a] of pure compounds at $T = 298.15$ K.

Compund[b]	V_i (cm^3 mol^{-1})	$\alpha_p \times 10^{-3}$ K^{-1}	$\kappa_T \times 10^{-12}$ Pa^{-1}	V_i^*(cm^3 mol^{-1})	P_i^*(J cm^{-3})
1O1	69.67[c]	1.996[c]	2514.6[d]	49.02	478.1
2O2	104.74[e]	1.654[e]	1967[e]	76.57	469.1
3O3	137.68[f]	1.261[f]	1440[f]	106	440.7
4O4	170.45[g]	1.1336[g]	1205.9[g]	133.74	455.2
5O5	203.40[h]	1.027[h]	1067[h]	162.02	450.8
6O6	235.81[i]	0.906[j]	865[j]	192.01	471
8O8	302.09[k]	0.68[j]	580[j]	236.59	485
1O2O1	104.34[c]	1.268[l]	1114.5[l]	80.25	573.4
2O2O2	141.33[m]	1.225[m]	1140.5[m]	109.38	534.6
1O1O1	89.49[n]	1.495[n]	1485[n]	66.3	574.2
2O1O2	126.38[n]	1.281[n]	1411[n]	97.0	465.3
1O2O2O1	142.93[l]	1.060[l]	821.6[l]	118.25	610.6
2O2O2O2	179.56[o]	1.11[o]	909.9[o]	141.4	586.5
THF	81.76[p]	1.2265[p]	962.3[p]	63.26	634.7
THP	98.19[c]	1.156[q]	990[r]	76.78	569.4
1,3-Dioxolane	69.98[s]	1.164[s]	758.3[s]	54.65	750.3
1,3-Dioxane	85.64[t]	1.05[t]	733[t]	68.08	675.7
1,4-Dioxane	85.71[c]	1.115[c]	738[c]	67.44	727.5
Benzene	89.44[c]	1.213[c]	966[c]	69.34	622.8
Toluene	106.89[c]	1.067[c]	912[c]	84.74	554.9

[a] V_i, molar volume, α_p, isobaric thermal expansion coefficient; κ_T, isothermal compressibility; V_i^*, reduction parameter for volume and P_i^*, reduction parameter for pressure.
[b] The figures represent the number of aliphatic groups attached to the O atoms, e.g. 1O1 is dimethylether and 1O2O2O1 is 2,5,8-trioxanonane; THF, tetrahydrofuran; THP, tetrahydropyran.
[c] [65].
[d] Estimated according to the method reported in Ref. [66].
[e] [67].
[f] [68].
[g] [69].
[h] [70].
[i] [71].
[j] Estimated value.
[k] [44].
[l] [72].
[m] [73].
[n] [74].
[o] [75].
[p] [76].
[q] [77].
[r] [78].
[s] [79].
[t] [56].

(10) and the mentioned $H^E_{m,exp}$ values at $\Delta x_1 = 0.05$. The X_{12} (x_1) variation is estimated from the equation:

$$\Delta_i = \frac{\left|\Delta X_{12}\right|_i^{max}}{X_{12}(x_1 = 0.5)} \quad (13)$$

where $\left|\Delta X_{12}\right|_i^{max}$ is the maximum absolute value of the $X_{12}(x_1) - X_{12}(x_1 = 0.5)$difference in the ranges [0.05, 0.45] ($i = 1$) and [0.55, 0.95] ($i = 2$). The corresponding values are listed in Table 4 (see also Figs. 5–7).

5. Discussion

Previously, it has been already pointed out that, in oxaalkane + aromatic compound mixtures, specific interactions of the n–π type between unlike molecules exist [31–33]. Thus, the exothermic H^E_m values of the 2,5-dioxahexane + benzene system [34] could be explained on the basis of such interactions. In order, to evaluate the strength of the ether–aromatic interactions, a method widely applied is the following [35–37]. Let us denote the positive contributions to H^E_m from the disruption of the ether–ether and aromatic–aromatic interactions by ΔH_{O-O} and $\Delta H_{aro-aro}$, respectively, and by ΔH_{O-aro}, the negative contribution from the creation of the ether–aromatic interactions. Then, we can write:

$$H^E_m = \Delta H_{O-O} + \Delta H_{aro-aro} + \Delta H_{O-aro} \quad (14)$$

This equation can be extended to $x_1 \to 0$ [38,39] to evaluate ΔH_{O-aro}, the strength of the interactions between ether and the aromatic compound in the studied solutions. In such case, ΔH_{O-O} and $\Delta H_{aro-aro}$ can be replaced by $H_1^{E,\infty}$ (partial excess molar enthalpy at infinite dilution of the first component) of ether or benzene, or toluene + alkane systems. Thus,

$$\Delta H_{O-aro} = H_1^{E,\infty}(\text{ether} + \text{aromatic compound}) - H_1^{E,\infty}(\text{ether} + \text{alkane}) - H_1^{E,\infty}(\text{aromatic compound} + \text{alkane}) \quad (15)$$

In mixtures with linear ethers, the considered alkane is heptane, while in cyclic ether solutions is cyclohexane. Table 5 lists ΔH_{O-aro} values for some selected mixtures. Below, we are referring to values of the excess functions at equimolar composition and 298.15 K.

5.1. $CH_3(CH_2)_{u-1}O(CH_2)_{u-1}CH_3$ + benzene

Here, H^E_m increases with u (Table 2). This may be explained on the basis of the following effects. (i) A weakening of the ether–benzene interactions, as the decrease of the $\left|\Delta H_{O-aro}\right|$ term for increased

Table 2
Molar excess enthalpies, H^E_m, at 298.15 K and equimolar composition for ether + benzene, or + toluene systems. The Flory interaction parameter, X_{12}, calculated from H^E_m at equimolar compostion, and the interactional and equation of state contributions, $H^E_{m,\,int}$ and $H^E_{m,\,EOS}$, respectively, are also included.

Ether[a]	H^E_m (J mol^{-1})	X_{12} (J cm^{-3})	$H^E_{m,int}$ (J mol^{-1})	$H^E_{m,EOS}$ (J mol^{-1})	$\sigma_r(H^E_m)$[b]	Ref.
Solvent: benzene						
1O1	−194[c]	−8.23	−82	−112	0.081	[80]
2O2	−8.7	0.772	10.8	−19.6	1.30	[81]
3O3	175	7.28	128	47	0.157	[82]
4O4	320	11.63	238	82	0.125	[83]
	304[d]	10.97	220	84	0.129	[84]
5O5	403	13.33	308	95	0.142	[71]
6O6	425	13.36	345	80	0.135	[71]
1O2O1	−179	−8.84	−130	−49	0.036	[34]
2O2O2	−281	−11.46	−207	−75	0.010	[71]
1O2O2O1	−286	−9.78	−193	−93	0.057	[82]
2O2O2O2	−428	−14.95	−318	−110	0.069	[82]
1O1O1	56	3.59	46	10	0.067	[85]
2O1O2	72	3.19	53	19	0.280	[85]
THF	−364	−21.16	−268	−96	0.029	[31]
THP	−253	−12.93	−187	−66	0.052	[86]
1,3-Dioxolane	79	4.53	52	17	0.670	[87]
1,3-Dioxane	−157	−8.47	−114	−43	0.104	[32]
1,4-Dioxane	−31	−1.63	−21.7	−9.3	7.3	[32]
Solvent: toluene						
1O1	−221[c]	−7.25	−78	−143	0.011	[80]
4O4	80[e]	2.72	61	19	0.136	[88]
THF	−363	−19.69	−269	−94	0.030	[58]
THP	−250	−11.96	−187	−63	0.082	[58]
1,3-Dioxolane	184	11.32	139	45	0.103	[58]
1,4-Dioxane	122	6.45	92	30	0.178	[58]

[a] For symbols, see Table 1.
[b] Eq. (12).
[c] T = 323.15 K.
[d] T = 313.15 K.
[e] T = 303.15 K.

u values indicates, which predominates over the lower positive $\Delta H_{O\text{–}O}$ contribution (Table 5). This is due to the decrease of the effective dipole moment, $\bar{\mu}$ [40–42], of the ether: 0.599 (u = 1) > 0.488 (u = 2) > 0.393 (u = 3) > 0.353 (u = 4) > 0.323 (u = 5) [42]. Note that interactions of the type dipole-induced dipole, like ether–benzene, can be represented by an average potential proportional to $\alpha_i\mu_j^2$ and inversely proportional to r^6 (α_i is the polarizability of the non-polar compound (benzene); μ_j is the dipole moment of the polar component (ether) and r is the intermolecular distance) [43]. Therefore, one could expect then that the higher $\bar{\mu}$ of the oxaalkane is, the stronger are the interactions between unlike molecules and also those between ether molecules

Table 3
Molar excess volumes, V^E_m at 298.15 K and equimolar composition for ether + benzene or + toluene systems. Comparison of experimental (exp.) results with Flory calculations.

System[a]	V^E_m(cm^3 mol^{-1})		Ref.
	Exp.	Flory	
4O4 + benzene	0.1298	0.375	[83]
	0.158		[89]
	0.158		[90]
1O2O1 + benzene	−0.017	−0.154	[34]
THF + benzene	−0.252	−0.254	[91]
	−0.253		[92]
	−0.216		[93]
THP + benzene	−0.166	−0.166	[91]
	−0.163		[94]
1,3-Dioxane + benzene	−0.191		[94]
	−0.200		[95]
1,4-	−0.065	−0.078	[94]
Dioxane + benzene	−0.065		[95]
4O4 + toluene	−0.153	−0.012[b]	[96]
THF + toluene	−0.369	−0.198	[97]
	−0.344		[93]
	−0.367		[98]
THP + toluene	−0.162	−0.162	[97]
	−0.159		[98]
1,3-Dioxolane + toluene	−0.124	0.208	[98]
1,4-Dioxane + toluene	−0.015	−0.015	[98]

[a] For symbols, see Table 1.
[b] Calculated at 303.15 K.

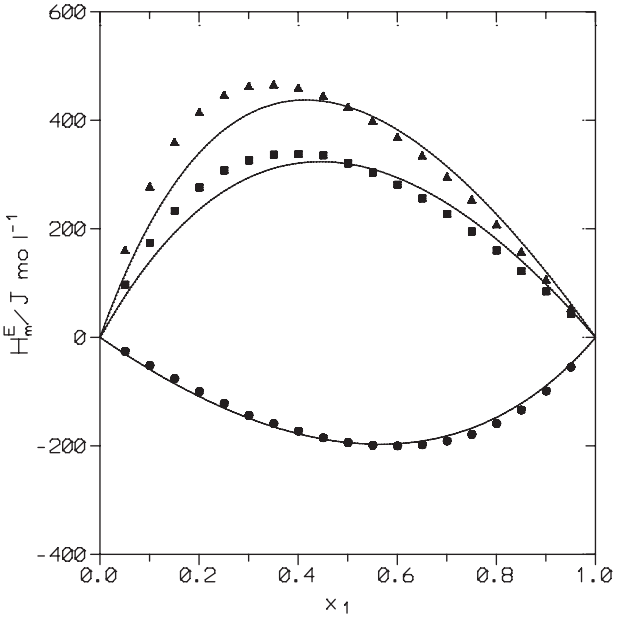

Fig. 1. H^E_m for linear monoether (1) + benzene (2) mixtures. Points, experimental results: (●) dimethylether (T = 323.15 K) [80]; (■) dibutylether (T = 298.15 K) [83]; (▲) dihexylether (T = 298.15 K) [71]. Solid lines, Flory calculations.

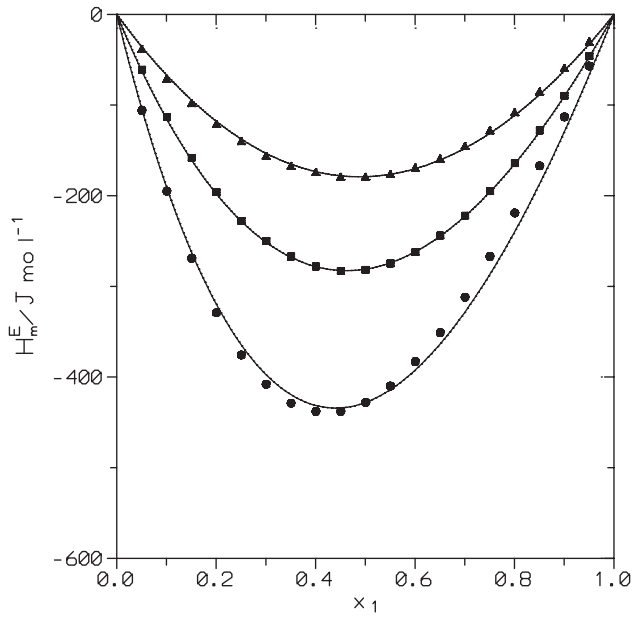

Fig. 2. H_m^E for linear polyether (1) + benzene (2) at 298.15 K. Points, experimental results: (▲) 2,5-dioxahexane [34]; (■) 3,6-dioxaoctane [71]; (●) 3,6,8-trioxaundecane [82]. Solid lines, Flory calculations.

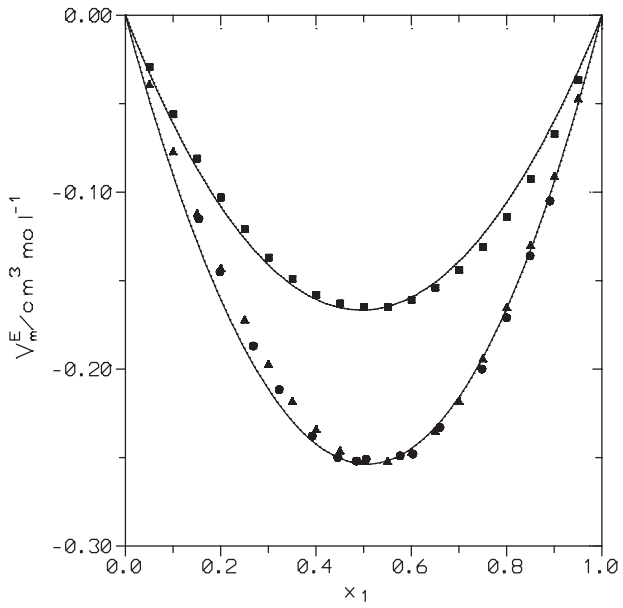

Fig. 4. V_m^E for cyclic monoether (1) + benzene (2) mixtures at 298.15 K. Points, experimental results: (●) [92] or (▲) [91], tetrahydrofuran; (■) tetrahydropyran [91]. Solid lines, Flory calculations.

(larger ΔH_{O-O} values, Table 5). (ii) Moreover, interactions between unlike molecules are less probable for mixtures with ethers of larger u values as their etheric surface is smaller, and it is more sterically hindered by the longer adjacent alkyl groups (steric effect). On the other hand, a higher positive $\Delta H_{aro-aro}$ contribution is expected due to the larger aliphatic surface of these ethers. Note that H_m^E of benzene + n-alkane increases with the chain length of the alkane (Table A.1, Appendix A).

It is remarkable that, although $X_{12}(x_1 = 0.5)$ increases with u (Table 2), solutions including ethers with $u = 5$ or 6 are characterized by close $X_{12}(x_1 = 0.5)$ values. This suggests that the mentioned systems mainly differ by geometrical factors. We have used $X_{12}(x_1 = 0.5) = 13.36\,J\,cm^{-3}$ (the value for the solution containing dihexyl ether) to predict V_m^E of the system with dioctyl ether. The result ($0.506\,cm^3\,mol^{-1}$) is in reasonable agreement with the experimental one ($0.550\,cm^3\,mol^{-1}$ [44]). It seems that the so-called Patterson effect [45], an extra positive contribution to H_m^E from the disruption of the order in longer n-alkanes by globular or plate like shape molecules, such benzene or cyclohexane [45,46], is not present in these systems.

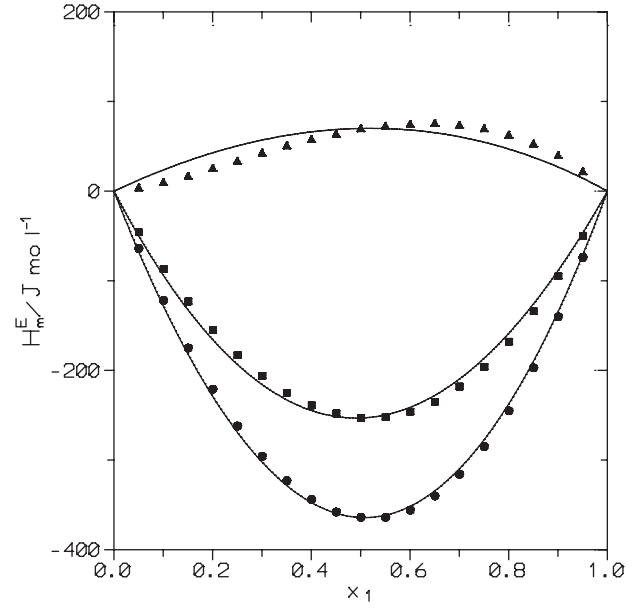

Fig. 3. H_m^E for cyclic ether (1) + benzene (2) mixtures at 298.15 K. Points, experimental results: (●) tetrahydrofuran [31]; (■) tetrahydropyran [86]; (▲) 1,3-dioxolane [87]. Solid lines, Flory calculations.

Table 4
Variations of the X_{12} values, Δ_i, obtained from H_m^E data at 298.15 of ether + benzene, or + toluene mixtures in the concentration ranges [0.05, 0.5] ($i = 1$) and [0.5, 0.95] ($i = 2$) calculated according to Eq. (13).

System[a]	Δ_1	Δ_2	Ref.
1O1 + benzene	0.222[b]	0.214[b]	[80]
2O2 + benzene	3.74	2.63	[81]
3O3 + benzene	0.184	0.255	[82]
4O4 + benzene	0.282	0.152	[83]
	0.278[c]	0.189[c]	[84]
5O5 + benzene	0.331	0.211	[71]
6O6 + benzene	0.373	0.140	[71]
1O2O1 + benzene	0.070	0.081	[34]
2O2O2 + benzene	0.012	0.022	[71]
2O2O2O2 + benzene	0.030	0.151	[82]
1O1O1 + benzene	0.042	0.061	[85]
2O1O2 + benzene	0.511	0.354	[85]
THF + benzene	0.050	0.039	[31]
THP + benzene	0.075	0.073	[86]
1,3-Dioxolane + benzene	0.675	0.534	[87]
1,3-Dioxane + benzene	0.107	0.200	[32]
1,4-Dioxane + benzene	2.38	1.77	[32]
1O1 + toluene	0.030[b]	0.052[b]	[80]
4O4 + toluene	0.195[d]	0.250[d]	[88]
THF + toluene	0.013	0.067	[58]
THP + toluene	0.010	0.022	[58]
1,3-Dioxolane + toluene	0.219	0.081	[58]
1,4-Dioxane + toluene	0.307	0.203	[58]

[a] For symbols, see Table 1.
[b] Data at 323.15 K.
[c] Data at 313.15 K.
[d] Data at 303.15 K.

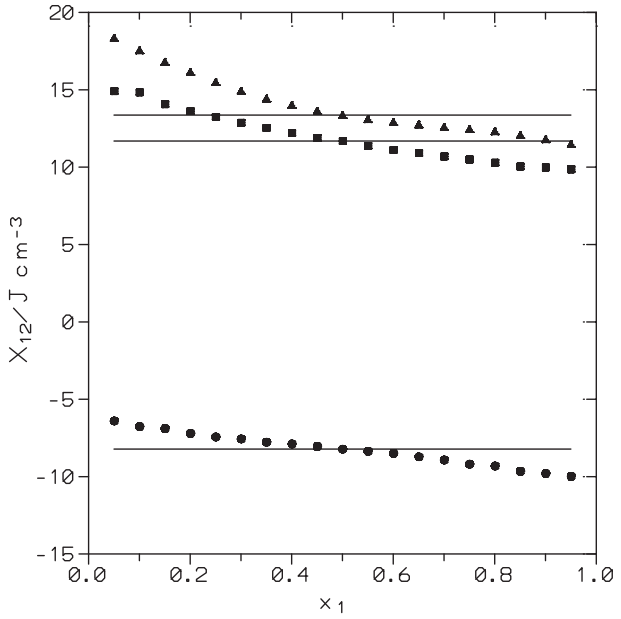

Fig. 5. Flory interaction parameters, X_{12}, for linear monoether (1) + benzene (2) mixtures. Points, values determined from H^E_m at $\Delta x_1 = 0.05$: (●) dimethylether (T = 323.15 K) [80]; (■) dibutylether (T = 298.15 K) [83]; (▲) dihexylether (T = 298.15 K) [71]. Solid lines, X_{12} values calculated from H^E_m at $x_1 = 0.5$.

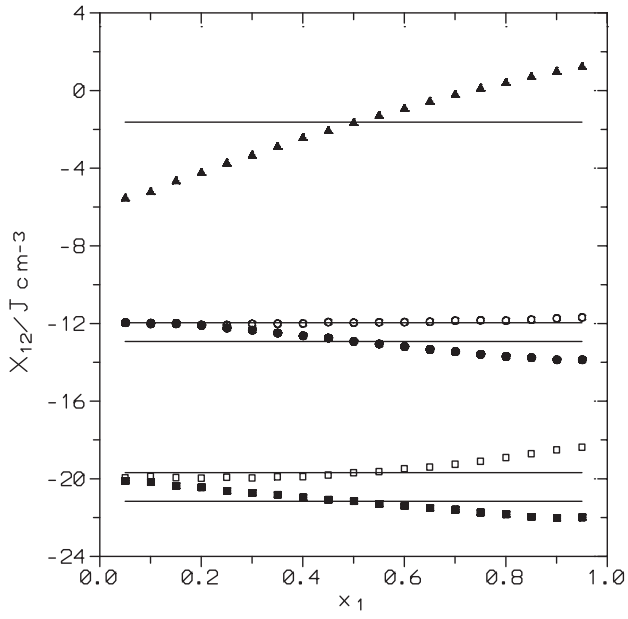

Fig. 7. Flory interaction parameters, X_{12}, for cyclic ether (1) + benzene (2), or + toluene (2) mixtures at 298.15 K. Points, values determined from H^E_m at $\Delta x_1 = 0.05$: (●) tetrahydrofuran + benzene [31]; (■) tetrahydropyran + benzene [86]; (▲) 1,4-dioxane + benzene [32]; (□) tetrahydrofuran + toluene [58]; (○) tetrahydropyran + toluene [58]. Solid lines, X_{12} values calculated from H^E_m at $x_1 = 0.5$.

The $\sigma_r(H^E_m)$ values determined from the Flory model for $CH_3(CH_2)_{u-1}O(CH_2)_{u-1}CH_3$ + heptane mixtures, are 0.053 (u = 2); 0.021 (u = 3); 0.020 (u = 3); 0.059 (u = 5) [16]; while $\sigma_r(H^E_m)$ = 0.047 for the benzene + octane system (Table A.1, Appendix A). The $\sigma_r(H^E_m)$ results for the present solutions are higher (Table 2), indicating that orientational effects are stronger. However, the rather moderate $\sigma_r(H^E_m)$ values obtained suggest that these effects are weak, which is supported by low C^E_{pm} negative values. So, for the dibutylether system, $C^E_{pm} \approx -1\,J\,mol^{-1}\,K^{-1}$, value calcu-

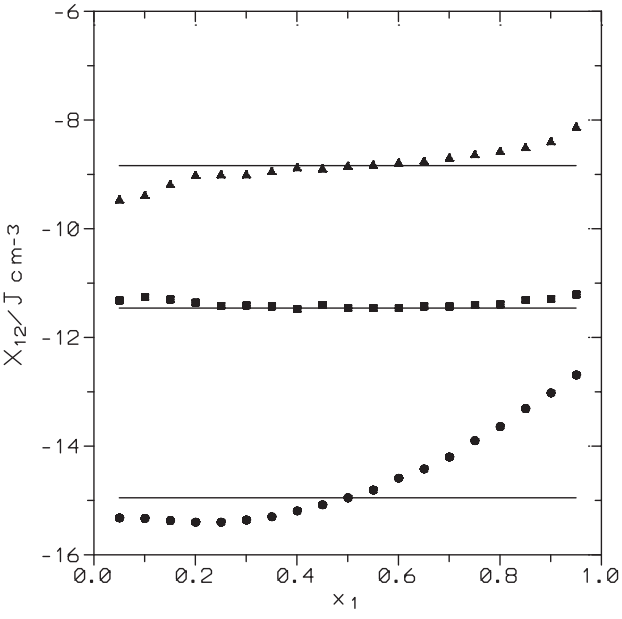

Fig. 6. Flory interaction parameters, X_{12}, for linear polyether (1) + benzene (2) mixtures at 298.15 K. Points, values determined from H^E_m at $\Delta x_1 = 0.05$: (▲) 2,5-dioxahexane [34]; (■) 3,6-dioxaoctane [71]; (●) 3,6,8-trioxaundecane [82]. Solid lines, X_{12} values calculated from H^E_m at $x_1 = 0.5$.

Table 5
Partial excess molar enthalpies at infinite dilution of the first compound, $H_1^{E,\infty}$, at T = 298.15 K for solute (1) + organic solvent (2) mixtures, and enthalpy of aromatic–ether interaction, $\Delta H_{(aromatic-O)}$, for ether (1) + aromatic compound (2) systems.

System[a]	$H_1^{E,\infty}$/kJ mol^{-1}	$\Delta H_{(aromatic-O)}$/kJ mol^{-1}
C_6H_6 + n-C_7	3.66 [99]	
C_6H_6 + n-C_6[b]	3.97 [100]	
C_6H_6 + C_6H_{12}	3.74 [101]	
C_7H_8 + C_6H_{12}	2.10 [102]	
1O1 + n-C_{10}[b]	1.92 [80]	
2O2 + n-C_7	1.60 [103]	
3O3 + n-C_7	0.84 [104]	
4O4 + n-C_7	0.531 [105]	
5O5 + n-C_7	0.496 [70]	
1O2O + n-C_7	5.48 [50]	
2O2O2 + n-C_7	4.53 [49]	
2O1O2 + n-C_7	2.42 [85]	
THF + C_6H_{12}	3.37 [58]	
THP + C_6H_{12}	2.22 [58]	
1,3-Dioxolane + C_6H_{12}	8.99 [58]	
1,3-Dioxane + C_6H_{12}	7.74 [32]	
1,4-Dioxane + C_6H_{12}	7.85 [32]	
1O1 + C_6H_6[b]	−0.535 [80]	−6.11
2O2 + C_6H_6	0.246 [81]	−5.01
3O3 + C_6H_6	1.15 [82]	−3.35
4O4 + C_6H_6	2.17 [83]	−2.02
5O5 + C_6H_6	2.92 [71]	−1.23
1O2O1 + C_6H_6	−0.815 [34]	−9.95
2O2O2 + C_6H_6	−1.25 [71]	−9.44
2O1O2 + C_6H_6	0.525 [85]	−5.45
THF + C_6H_6	−1.40 [91]	−8.51
THP + C_6H_6	−0.816 [91]	−6.78
1,3-Dioxane + C_6H_6	−0.694 [32]	−12.17
1,4-Dioxane + C_6H_6	−0.444 [32]	−12.03
THF + C_7H_8	−1.33 [58]	−6.8
THP + C_7H_8	−0.98 [58]	−5.3
1,3-Dioxolane + C_7H_8	0.463 [58]	−10.63
1,4-Dioxane + C_7H_8	0.206 [58]	−9.74

[a] For symbols, see Table 1.
[b] T = 323.15 K.

lated from H^E_m data at 298.15 K and 313.15 K (see Table 2). Negative C^E_{pm} values are typical of mixtures characterized by dispersive interactions (e.g., $C^E_{pm} = -3.34\,J\,mol^{-1}\,K^{-1}$ for the benzene + heptane system [47]). On the other hand, Table 4 reveals that orientational effects are more important at $x_1 < 0.5$, where $X_{12}(x_1) > X_{12}(x_1 = 0.5)$ and the model overestimates interactions between unlike molecules. The opposite trend is encountered at $x_1 > 0.5$. In $CH_3(CH_2)_{u-1}O(CH_2)_{u-1}CH_3$ or benzene + *n*-alkane mixtures, orientational effects are more relevant at low concentration of the ether and at high concentration of benzene, respectively. This could explain the large values (Table 4). The large $\sigma_r(H^E_m)$ and Δ_i values obtained for the diethylether mixture merely reflects that the model can not represent very asymmetric curves, as s-shaped ones, when the mixture compounds show close V_i and V_i^* values. The same occurs for the 1,4-dioxane + benzene system. This is a shortcoming of the model.

5.2. Linear polyether or acetal + benzene

The replacement of a linear monoether by a linear polyether of similar size leads to a H^E_m decrease which may be ascribed to interactions between unlike molecules become stronger in the latter mixtures (higher $|\Delta H_{O-aro}|$ values, Table 5), in such way that the more negative ΔH_{O-aro} contribution is prevalent over the more positive ΔH_{O-O} term. This is consistent with the higher $\bar{\mu}$ values of polyethers in comparison to those of monoethers. For example, $\bar{\mu}$ (2,5-dioxahexane) = 0.653 [42]. The stronger ether–ether interactions in systems with polyethers are also supported by the fact that, at 298.15 K, the systems 2,5,8,11-tetraoxadodecane + dodecane or 2,5,8,11,14-pentaoxapentadecane + decane are close to their upper critical solution temperatures (280.81 K and 291.98 K respectively [48]). In addition, the larger etheric surface of polyethers makes easier the creation of the new ether–aromatic interactions upon mixing.

H^E_m of solutions including $CH_3(CH_2)_{u-1}O(CH_2CH_2O)_v(CH_2)_{u-1}CH_3$, decreases when u is increased for a given v value (Table 2). In the case of the longer ethers, this may be ascribed to a lower ΔH_{O-O} contribution to H^E_m and not to stronger ether–benzene interactions. In fact, $\bar{\mu}$ (3,6-dioxaoctane) = 0.525 [42]; in heptane solutions $H^E_m(J\,mol^{-1}) = 889$ (3,6-dioxaoctane) [49] <1285 (2,5-dioxahexane) [50], and ΔH_{O-O} (kJ mol^{-1}) = 4.53 (3,6-dioxaoctane), <5.48 (2,5-dioxahexane) (Table 5). Similarly it may be explained the observed decrease of H^E_m when v is increased for a fixed u value.

It is known that proximity effects lead to a weakening of the interactions between ether molecules in mixtures with alkanes [51], as $\bar{\mu}$ (acetal) < $\bar{\mu}$ (diether) (e.g., $\bar{\mu}$ (3,5-dioxaheptane) = 0.421 [42]) and then ΔH_{O-O} (3,6-dioxaoctane) > ΔH_{O-O} (3,5-dioxaheptane) = 2.42 kJ mol^{-1} (Table 5). In solutions containing benzene, interactions between unlike molecules also become weaker when an acetal in replaced by a diether of similar size (Table 5). In this case, the lower $|\Delta H_{O-aro}|$ term overcompensates the decrease of the ΔH_{O-O} contribution and H^E_m increases (Table 2).

For linear polyether + heptane systems, we have previously obtained using Flory $\sigma_r(H^E_m) = 0.055$ (2,5-dioxahexane); 0.065 (2,5,8-trioxanonane); 0.065 (3,6-dioxaoctane); 0.058 (2,4-dioxapentane); 0.039 (3,5-dioxaheptane) = 0.039 [16]. These results are similar to those determined here for the benzene solutions (Table 2). Therefore, it may be concluded that the mixture structure is newly close to random mixing. Note that the Δ_i values are lower than for the systems with linear monoethers (Table 4). The observed discrepancies for the 3,5-dioxaheptane + benzene mixture may be related to experimental inaccuracies as the H^E_m curve is very shifted towards low x_1 values of the acetal when is compared to that of the 2,4-dioxapentane solution.

5.3. Cyclic ether + benzene

For monoethers, cyclization, that is, the replacement of a linear ether by a homomorphic cyclic one, also implies decreased H^E_m values, which may be explained in the same terms as above. Ether–benzene interactions are stronger in solutions with cyclic ethers, and the more negative ΔH_{O-aro} (Table 5) contribution is prevalent over the more positive ΔH_{O-O} term. This is due to the $\bar{\mu}$ values of tetrahydrofuran, 0.723, and of tetrahydropyran, 0.619, are larger than those of homomorphic linear ethers [42], and to the oxygen atom is less sterically hindered in cyclic molecules. Systems with diethers behave differently, depending on the considered oxaalkane. Note that $H^E_m(J\,mol^{-1}) = -31$ (1,4-dioxane) [32] >−179 (2,5-dioxahexane) [34], which might be due to the ΔH_{O-O} contribution becomes here more relevant. However, this seems to be no the case for the 1,3-dioxane mixture as the corresponding H^E_m value (−157 J mol^{-1} [32] is expected to be lower than that of the homomorphic acetal. (See H^E_m values for mixtures with 2,4-dioxapentane, or 3,5-dioxaheptane listed in Table 2.) This merely remarks the complex behaviour of systems with cyclic diethers. In terms of the classical UNIFAC model, it has been shown, on the basis on principles of unchanging geometry and approximate group electroneutrality, that new groups must be introduced to a correct description of systems with cyclic ethers [52–54]. A similar conclusion has been stated using DISQUAC [16,55].

Results from the Flory model for heptane mixtures are: $\sigma_r(H^E_m) =$ 0.064 (tetrahydrofuran); 0.062 (tetrahydropyran); 0.094 (1,3-dioxolane); 0.159 (1,3-dioxane); 0.071 (1,4-dioxane) [16]. For the systems with benzene, $\sigma_r(H^E_m)$ substantially differs for systems including cyclic monoethers or cyclic diethers. For the former, orientational effects are weak, as it is indicated by low $\sigma_r(H^E_m)$ and Δ_i values (Tables 2 and 4), and then the random mixing hypothesis may be considered to be valid to a large extent. In contrast, the model predicts strong orientational effects in systems with 1,3-dioxolane or 1,4-dioxane. However, such effects are weak as it is revealed by low $|H^E_m|$ (Table 2) and C^E_{pm} values. So, $C^E_{pm}(J\,mol^{-1}\,K^{-1}) = 1.18$ (1,3-dioxolane), 0.41 (1,4-dioxane) [33]. Moreover, the corresponding molar excess isochoric heat capacities, C^E_{Vm}, are also low and positive, 0.70 and 0.55 J mol^{-1} K^{-1}, respectively [56]. This allows to conclude that the random mixing hypothesis is also a reasonable approximation for such solutions as, in terms of the Flory theory, $C^E_{Vm} = 0$ [57].

5.4. Ether + toluene

Ether–aromatic interactions are weaker in toluene mixtures, as the formation of such interactions is more difficult due to the smaller aromatic surface of toluene (Table 5). This means an increase of H^E_m which, in systems with cyclic monoethers, seems to be compensated by the decrease related to a lower $\Delta H_{aro-aro}$ contribution in such way that H^E_m is practically independent of the aromatic compound, benzene or toluene. For cyclic diether + toluene systems H^E_m is higher as the decrease of the $|\Delta H_{O-aro}|$ term is not compensated by the lower $\Delta H_{aro-aro}$ contribution.

The $\sigma_r(H^E_m)$ values show that the orientational effects are weak and that the mixture structure is here also similar to that of the systems examined above. Accordingly, C^E_{pm} is low for these solutions (1.59, 1.34, 1.98 and 1.10 J mol^{-1} K^{-1} for the systems with tetrahydrofuran tetrahydropyran, 1,3-dioxolane and 1,4-dioxane, respectively [58].

Finally, it should be mentioned that the Kirkwood–Buff formalism [59–61] has been applied to determine the Kirkwood–Buff integrals, G_{ij}, and related magnitudes as linear coefficients of preferential solvation, δ_{ij}, or local mole fractions, x_{ij}, for tetrahydrofuran

Table A.1
Molar excess enthalpies, H^E_m, at 298.15 K and equimolar composition for benzene + *n*-alkane systems. The Flory interaction parameter X_{12} calculated from H^E_m at equimolar compostion, the interactional contribution, $H^E_{m,int}$, and variations of the X_{12} values, Δ_i (Eq. (13)), obtained from H^E_m data at 298.15 are also included.

Alkane[a]	H^E_m(J mol^{-1})	X_{12} (J cm^{-3})	$H^E_{m,int}$(J mol^{-1})	$\sigma_r(H^E_m)$[b]	Δ_1	Δ_2
Hexane[c]	897	43.64	644	0.026	0.054	0.022
Octane[d]	969	44.13	710	0.047	0.048	0.098
Dodecane[d]	1101	46.90	846	0.063	0.073	0.102
Hexadecane[d]	1256	51.26	992	0.177	0.070	0.176

[a] Flory parameters for pure alkanes are taken from [3].
[b] Eq. (12).
[c] L. Romaní, M.I. Paz-Andrade, An. Quim. 70 (1974) 422–425.
[d] M. Díaz Peña, C. Menduiña, J. Chem. Thermodyn. 6 (1974) 387–393.

or 1,4-dioxane + benzene, or +toluene mixtures [32,62,63]. The low $|G_{ij}|$ and $|\delta_{ij}|$ values obtained lead to x_{ij} values which are very close to the bulk ones. Thus, the main conclusion of these studies is that such solutions hardly show any preferential solvation [32,62,63], which confirms our conclusions.

5.5. Molar excess volumes

For most of the systems listed in Table 3, V^E_m is negative indicating that the negative contributions to this excess function from interactions between unlike molecules and/or from structural effects are predominant over the positive contribution from the breaking of interactions between like molecules. We note that both magnitudes H^E_m and V^E_m show the same sign (negative) and change in the same sequence for cyclic ether + benzene mixtures: tetrahydrofuran < tetrahydropyran < 1,3-dioxane < 1,4-dioxane. This suggests that the contribution to V^E_m from interactions between unlike molecules is the more important. In contrast, H^E_m and V^E_m are both positive for dibutyl, or dioctyl ether + benzene systems, and the contribution to V^E_m from the disruption of interactions between like molecules becomes predominant For 1,3-dioxolane or 1,4-dioxane + toluene, $H^E_m > 0$ and $V^E_m < 0$, which points out that here structural effects are more relevant.

The observed discrepancies between experimental and calculated values could be rather easily analyzed in terms of the Prigogine–Flory version of the theory [64]. In this version of the model, the curvature term of V^E_m is proportional to $-(\tilde{V}_1 - \tilde{V}_2)^2$, and the so-called P^* term is proportional to $(P^*_1 - P^*_2)(\tilde{V}_1 - \tilde{V}_2)$. Inspection of Table 3 shows that large discrepancies between theory and experiment are usually encountered when the P^* term is high in absolute value as for dibutylether + benzene, or tetrahydrofuran 1,3-dioxolane or 1,4-dioxane + toluene mixtures. In this case, the P^* contribution is positive and the theoretical V^E_m is higher than the experimental value. For the 2,5-dioxahexane, or 1,4-dioxane + benzene mixtures, the mentioned contribution is negative and the Flory results are lower than the experimental ones.

6. Conclusions

The relative variation of H^E_m, along homologous series, for ether + benzene, or + toluene systems has been discussed taking into account the contributions to H^E_m from ether–ether, aromatic–aromatic and ether–aromatic interactions. It has been shown that the increase of u (v fixed) in $CH_3(CH_2)_{u-1}O(CH_2CH_2O)_v(CH_2)_{u-1}CH_3$ + benzene mixtures leads to a weakening of interactions between unlike molecules. These interactions are also weakened by proximity effects. In contrast, the v increase (u fixed) or cyclization lead to stronger interactions between unlike molecules. From the application of the Flory model, it is concluded that orientational effects are weak in the investigated systems, in such way that the mixture structure is close to random mixing. The theory predicts strong orientational effects for 1,3-dioxolane, or 1,4-dioxane + benzene solutions, but this has been attributed to the theory cannot describe asymmetric H^E_m curves when the mixture compounds show close V_i and V^*_i values. Conclusions are confirmed by previous calculations on the basis of the Kirkwood–Buff integrals formalism.

7. List of symbols

C_p	heat capacity at constant pressure
H	molar enthalpy
ΔH	contribution to the molar excess enthalpy (three types are considered; ether–ether, aromatic–aromatic and ether–aromatic)
P	pressure
P^*	reduction parameter for pressure in the Flory theory
T	temperature
T^*	reduction parameter for temperature in the Flory theory
V	molar volume
V^*	reduction parameter for volume in the Flory theory
x	mole fraction
X_{12}	interaction parameter in the Flory theory

Greek letters

$\tilde{\mu}$	effective dipole moment
σ_r	relative standard deviation (Eq. (12))

Superscripts

E	excess property
∞	property at infinite dilution

Subscripts

i	mixture compound (i = 1,2)
m	molar property

Acknowledgements

The authors gratefully acknowledge the financial support received from the Consejería de Educación y Cultura of Junta de Castilla y León, under the Project VA052A09 and from the Ministerio de Educación y Ciencia, under the Project FIS2010-16957.

Appendix A.

See Table A.1.

References

[1] P.J. Flory, J. Am. Chem. Soc. 87 (1965) 1833–1838.
[2] E. Aicart, C. Menduiña, R.L. Arenosa, G. Tardajos, J. Solution Chem. 12 (1983) 703–716.
[3] N. Riesco, J.A. González, S. Villa, I. García de la Fuente, J.C. Cobos, Phys. Chem. Liq. 41 (2003) 309–321.

[4] L. Wang, G.C. Benson, B.C.-Y. Lu, Thermochim. Acta 213 (1993) 83–93.
[5] G.C. Benson, H.D. Pflug, J. Chem. Eng. Data 15 (1970) 382–386.
[6] N. Riesco, S. Villa, J.A. González, I. García de la Fuente, J.C. Cobos, Thermochim. Acta 362 (2000) 89–97.
[7] T.M. Letcher, W.L. Spiteri, J. Chem. Thermodyn. 11 (1979) 435–440.
[8] S.N. Battacharyya, D. Patterson, J. Phys. Chem. 83 (1979) 2979–2985.
[9] T.M. Letcher, J. Chem. Thermodyn. 16 (1984) 805–810.
[10] G. Tardajos, E. Aicart, M. Costas, D. Patterson, J. Chem. Soc. Faraday Trans. 1 (82) (1986) 2977–2987.
[11] G.C. Benson, C.J. Halpin, Can. J. Chem. 65 (1987) 322–325.
[12] E. Aicart, C. Menduiña, R.L. Arenosa, G. Tardajos, J. Solution Chem. 13 (1984) 443–455.
[13] J.A. González, I. Mozo, I. García de la Fuente, J.C. Cobos, N. Riesco, Thermochim. Acta 476 (2008) 20–27.
[14] J.A. González, N. Riesco, I. Mozo, I. García de la Fuente, J.C. Cobos, Ind. Eng. Chem. Res. 46 (2007) 1350–1359.
[15] J.A. González, N. Riesco, I. Mozo, I. García de la Fuente, J.C. Cobos, Ind. Eng. Chem. Res. 48 (2009) 7417–7429.
[16] J.A. González, Ind. Eng. Chem. Res. 49 (2010) 9511–9524.
[17] T. Iida, T. Endo, M.M. Ito, J. Phys. Org. Chem. 13 (2000) 330–336.
[18] J.F. Stoddart, Chem. Soc. Rev. 8 (1979) 85–142.
[19] R.W. Reynolds, J.S. Smith, T. Steinmetz, Abstracts of Papers of the American Chemical Society, 1974 p. 11.
[20] R. Csikos, J. Pallay, J. Laky, E.D. Radchenko, B.A. Englin, J.A. Robert, Hydrocarbon Process. Int. Ed. 55 (1976) 121–125.
[21] D.J. Cram, J.M. Cram, Science 183 (1974) 803–809.
[22] H.V. Kehiaian, Thermochemistry and Thermodynamics, MTP Int. Review of Science, Butterworths, London, 1972.
[23] R.M. Izatt, J.D. Lamb, N.E. Izatt, B.E. Rossiter, J.J. Christensen, B.L. Haymore, J. Am. Chem. Soc. 101 (1979) 6273–6276.
[24] J.D. Lamb, R.M. Izatt, C.S. Swain, J.J. Christensen, J. Am. Chem. Soc. 102 (1980) 475–479.
[25] G. Pokol, B. Agai, T.M.T. Tran, I. Bitter, L. Töke, S. Gál, Thermochim. Acta 319 (1998) 87–95.
[26] A. Abe, P.J. Flory, J. Am. Chem. Soc. 87 (1965) 1838–1846.
[27] P.J. Flory, R.A. Orwoll, A. Vrij, J. Am. Chem. Soc. 86 (1974) 3507–3514.
[28] P.J. Flory, R.A. Orwoll, A. Vrij, J. Am. Chem. Soc. 86 (1964) 3515–3520.
[29] R.A. Orwoll, P.J. Flory, J. Am. Chem. Soc. 89 (1967) 6822–6829.
[30] P.J. Howell, B.J. Skillerne de Bristowe, D. Stubley, J. Chem. Soc. A (1971) 397–400.
[31] A. Inglese, E. Wilhelm, J.-P.E. Grolier, H.V. Kehiaian, J. Chem. Thermodyn. 13 (1981) 229–234.
[32] T. Takigawa, H. Ogawa, K. Tamura, S. Murakami, Fluid Phase Equilib. 136 (1997) 257–267.
[33] T. Takigawa, K. Tamura, H. Ogawa, S. Murakami, S. Takagi, Thermochim. Acta 352–353 (2000) 25–29.
[34] H. Ohji, K. Tamura, J. Chem. Thermodyn. 35 (2003) 1591–1599.
[35] H.P. Diogo, M.E. Minas de Piedade, J. Moura Ramos, J. Simoni, J.A. Martinho Simoes, J. Chem. Educ. 70 (1993) A227.
[36] T.M. Letcher, U.P. Govender, J. Chem. Eng. Data 40 (1995) 1097–1100.
[37] E. Calvo, P. Brocos, A. Piñeiro, M. Pintos, A. Amigo, R. Bravo, A.H. Roux, G.R. Desgranges, J. Chem. Eng. Data 44 (1999) 948–954.
[38] T.M. Letcher, B.C. Bricknell, J. Chem. Eng. Data 41 (1996) 166–169.
[39] J.A. González, I. Mozo, I. García de la Fuente, J.C. Cobos, N. Riesco, J. Chem. Thermodyn. 40 (2008) 1495–1508.
[40] J.S. Rowlinson, F.L. Swinton, Liquid and Liquid Mixtures, third ed., G.B., Butterworths, 1982.
[41] E. Wilhelm, A. Laínez, J.-P.E. Grolier, Fluid Phase Equilib. 49 (1989) 233–250.
[42] J.A. González, I. García de la Fuente, J.C. Cobos, Fluid Phase Equilib. 154 (1999) 11–31.
[43] J.M. Prausnitz, Molecular Thermodynamics of Fluid Phase Equilibria, Prentice-Hall, Englewood Cliffs, NJ, 1969.
[44] N.M. Djordjevic, Thermochim. Acta 143 (1989) 171–176.
[45] M. Costas, D. Patterson, Thermochim. Acta 120 (1987) 161–181.
[46] J.A. González, I. García de la Fuente, J.C. Cobos, C. Casanova, A. Ait-Kaci, Fluid Phase Equilib. 112 (1995) 63–87.
[47] J.-P.E. Grolier, A. Faradizadeh, H.V. Kehiaian, Thermochim. Acta 53 (1982) 157–162.
[48] T. Treszczanowicz, D. Cieslak, J. Chem. Thermodyn. 25 (1993) 661–665.
[49] G.C. Benson, M.K. Kumaran, P.J. D'Arcy, Thermochim. Acta 74 (1984) 187–191.
[50] M.K. Kumaran, G.C. Benson, J. Chem. Thermodyn. 18 (1986) 27–29.
[51] H.V. Kehiaian, M.R. Tiné, L. Lepori, E. Matteoli, B. Marongiu, Fluid Phase Equilib. 46 (1989) 131–177.
[52] H.S. Wu, S.I. Sandler, AIChE J. 25 (1989) 168–172.
[53] H.S. Wu, S.I. Sandler, Ind. Eng. Chem. Res. 30 (1991) 881–889.
[54] H.S. Wu, S.I. Sandler IInd, Eng. Chem. Res. 30 (1991) 889–897.
[55] J.A. González, I. Mozo, I. García de la Fuente, J.C. Cobos, V. Durov, Fluid Phase Equilib. 245 (2006) 168–184.
[56] T. Takigawa, K. Tamura, J. Chem. Thermodyn. 32 (2000) 1045–1055.
[57] A. Domínguez, G. Tardajos, E. Aicart, S. Pérez-Casas, L.M. Trejo, M. Costas, D. Patterson, H.V. Tra, J. Chem. Soc. Faraday Trans. 89 (1993) 89–93.
[58] P. Brocos, E. Calvo, R. Bravo, M. Pintos, A. Amigo, A.H. Roux, G. Roux-Desgranges, J. Chem. Eng. Data 44 (1999) 67–72.
[59] J.G. Kirkwood, F.P. Buff, J. Chem. Phys. 19 (1951) 774–777.
[60] A. Ben-Naim, J. Phys. Chem. 67 (1977) 4884–4890.
[61] E. Matteoli, L. Lepori, J. Chem. Phys. 80 (1984) 2856–2863.
[62] Y. Marcus, J. Mol. Liq. 128 (2006) 115–126.
[63] Y. Marcus, J. Solution Chem. 35 (2006) 251–277.
[64] L. Andreoli Ball, L.M. Trejo, M. Costas, D. Patterson, Fluid Phase Equilib. 147 (1998) 163.
[65] J.A. Riddick, W.B. Bunger, T.K. Sakano, Organic solvents, in: A. Weissberger (Ed.), Techniques of Chemistry, vol. II, Wiley, N.Y., 1986.
[66] G. Manzini, V. Crescenzi, G. Chim. Ital. 104 (1974) 51–61.
[67] J. Canosa, A. Rodríguez, J. Tojo, Fluid Phase Equilib. 156 (1999) 57–71.
[68] R. Garriga, S. Martínez, P. Pérez, M. Gracia, Fluid Phase Equilib. 147 (1998) 195–206.
[69] I. Mozo, I. García de la Fuente, J.A. González, J.C. Cobos, J. Mol. Liq. 129 (2006) 155–163.
[70] L. Wang, G.C. Benson, B.C.-Y. Lu, Fluid Phase Equilib. 46 (1989) 211–221.
[71] B. Marongiu, A. Piras, S. Porcedda, E. Tuveri, J. Thermal. Anal. Calorim. 95 (2009) 149–159.
[72] J. Peleteiro, C.A. Tovar, R. Escudero, S. Carballo, J.L. Legido, L. Romaní, J. Solution Chem. 22 (1993) 1005–1017.
[73] M.K. Kumaran, F. Kimura, C.J. Halpin, G.C. Benson, J. Chem. Thermodyn. 16 (1984) 687–691.
[74] T. Treszczanowicz, Thermochim. Acta 160 (1990) 253–266.
[75] A. Pal, S. Sharma, G. Dass, J. Chem. Thermodyn. 31 (1999) 273–287.
[76] M. Keller, S. Schnabel, A. Heintz, Fluid Phase Equilib. 110 (1995) 231–265.
[77] B. Giner, B. Olivares, I. Giner, G. Pera, C. Lafuente, J. Solution Chem. 36 (2007) 375–386.
[78] I. Cibulka, L. Hneskowsky, T. Takagi, J. Chem. Eng. Data 42 (1997) 2–26.
[79] I. Gascón, M.C. López, C. Lafuente, F.M. Royo, P. Cea, Thermochim. Acta 423 (2003) 49–85.
[80] S.-J. Park, K.-J. Han, J. Gmehling, J. Chem. Eng. Data 52 (2007) 1814–1818.
[81] J.-E.A. Otterstedt, W. Missen, J. Chem. Eng. Data 11 (1966) 360–361.
[82] H.V. Kehiaian, K. Sosnkowska-Kehiaian, R. Hryniewicz, J. Chim. Phys. Phys. -Chim. Biol. 68 (1971) 922–934.
[83] J.B. Ott, K.N. Marsh, A.E. Richards, J. Chem. Thermodyn. 13 (1981) 447–455.
[84] F. Aguilar, F.E.M. Alaoui, J.J. Segovia, M.A. Villamañán, E.A. Montero, Fluid Phase Equilib. 284 (2009) 106–113.
[85] R.J. Meyer, J. Metzger, C. Kehiaian, H.V. Kehiaian, Thermochim. Acta 38 (1980) 197–209.
[86] A.W. Andrews, K.W. Morcom, J. Chem. Thermodyn. 3 (1971) 519–525.
[87] R.J. Meyer, G.L. Giusti, M.F. Meyer, J. Chem. Thermodyn. 11 (1979) 713–718.
[88] S.C. Sharma, P. Kumar, M. Syngal, J. Chem. Thermodyn. 23 (1991) 43–47.
[89] J. George, N.V. Sastry, J. Chem. Thermodyn. 35 (2003) 1837–1853.
[90] K.-J. Han, I.-C. Hwang, I.-H. Park, J. Chem. Eng. Data 52 (2007) 1018–1024.
[91] B. Giner, S. Martín, H. Arrigas, M.C. López, C. Lafuente, J. Phys. Chem. B 110 (2006) 17683–17690.
[92] R. Meyer, G. Giusti, M. Meyer, E.-J. Vicent, Thermochim. Acta 13 (1975) 379–384.
[93] B.S. Mahl, Z.S. Kooner, J.R. Khurma, J. Chem. Eng. Data 23 (1978) 150–152.
[94] A.W. Andrews, K.W. Morcom, J. Chem. Thermodyn. 3 (1971) 513–518.
[95] T. Kimura, S. Takagi, Netsu Sokutei 24 (1997) 219–227.
[96] H.-Y. Kwak, J.-H. Oh, S.-J. Park, K.-Y. Paek, Fluid Phase Equilib. 262 (2007) 161–168.
[97] P. Brocos, A. Amigo, M. Pintos, E. Calvo, R. Bravo, Thermochim. Acta 286 (1996) 297–306.
[98] R. Francesconi, F. Comelli, J. Chem. Eng. Data 37 (1992) 230–232.
[99] E. Munsch, Thermochim. Acta 22 (1978) 237–255.
[100] M. Díaz Peña, C. Menduiña, J. Chem. Thermodyn. 6 (1974) 1097–1102.
[101] J.-P.E. Grolier, Thermochim. Acta 16 (1976) 27–38.
[102] K.-Y. Hsu, H.L. Clever, J. Chem. Thermodyn. 7 (1975) 435–442.
[103] L.G.C. Benson, B.C.-Y. Lu, J. Chem. Thermodyn. 20 (1988) 267–271.
[104] F. Kimura, P.J. D'Arcy, G.C. Benson, J. Chem. Thermodyn. 15 (1983) 511–516.
[105] G.C. Benson, B. Luo, B.C.-Y Lu, Can. J. Chem. 66 (1988) 531–534.